

ROBERT KOCH INSTITUT



Originally published as:

van Baarle, S., Celik, I.N., Kaval, K.G., Bramkamp, M., Hamoen, L.W., Halbedel, S.
Protein-protein interaction domains of *Bacillus subtilis* DivIVA
(2013) *Journal of Bacteriology*, 195 (5), pp. 1012-1021.

DOI: 10.1128/JB.02171-12

This is an author manuscript.

The definitive version is available at: <http://jb.asm.org/>

1 **Protein-protein interaction domains of *Bacillus subtilis* DivIVA**

2
3 Suey van Baarle^{2,3}, Ilkay Nazli Celik², Karan Gautam Kaval¹, Marc Bramkamp^{3,4}, Leendert
4 W. Hamoen^{2,5*}, and Sven Halbedel^{1,2*}

5
6 ¹ Robert Koch Institute, FG11 - Division of Bacterial Infections, Burgstrasse 37, 38855
7 Wernigerode, Germany;

8 ² Centre for Bacterial Cell Biology, Newcastle University, Richardson Road, NE2 4AX
9 Newcastle upon Tyne, United Kingdom;

10 ³ Institute for Biochemistry, University of Cologne, Zùlpicher Strasse 47, 50674 Cologne,
11 Germany;

12 ⁴ Department Biology I, Ludwig-Maximilians University Munich, Biozentrum, Großhaderner
13 Str. 2-4, 82152 Martinsried, Germany;

14 ⁵ Bacterial Cell Biology, Swammerdam Institute for Life Sciences (SILS) University of
15 Amsterdam, The Netherlands;

16
17 Key words: cell division, sporulation, coiled coil, protein localization, membrane curvature

18 Running title: DivIVA interaction domains

19
20 * corresponding authors:

21 halbedels@rki.de, Robert Koch Institute, FG11 - Division of Bacterial Infections, Burgstrasse
22 37, D-38855 Wernigerode, Germany; phone: +49-30-18754-4323; fax: +49-30-18754-4207;

23 l.w.hamoen@uva.nl, Bacterial Cell Biology, Swammerdam Institute for Life Sciences (SILS)
24 University of Amsterdam Science Park 904 (room C3.106), 1098 XH Amsterdam, The
25 Netherlands; phone: +31-205255115 or l.hamoen@ncl.ac.uk, Centre for Bacterial Cell

26 Biology, Newcastle University, Richardson Road, NE2 4AX Newcastle upon Tyne, United
27 Kingdom; phone: +44-191-2083240, fax: +44-191-222-7424

ABSTRACT

1
2 DivIVA proteins are curvature sensitive membrane binding proteins that recruit other proteins
3 to the poles and the division septum. They consist of a conserved N-terminal lipid binding
4 domain fused to a less conserved C-terminal domain. DivIVA homologues interact with
5 different proteins involved in cell division, chromosome segregation, genetic competence, or
6 cell wall synthesis. It is unknown how DivIVA interacts with these proteins, and we used the
7 interaction of *Bacillus subtilis* DivIVA with MinJ and RacA to investigate this. MinJ is a
8 trans-membrane protein controlling division site selection, and the DNA-binding protein
9 RacA is crucial for chromosome segregation during sporulation. Initial bacterial two-hybrid
10 experiments revealed that the C-terminus of DivIVA appears to be important for recruiting
11 both proteins. However, the interpretation of these results is limited since it appeared that C-
12 terminal truncations also interfere with DivIVA oligomerization. Therefore a chimera
13 approach was followed, making use of the fact that *Listeria monocytogenes* DivIVA shows
14 normal polar localization but is not biologically active when expressed in *B. subtilis*.
15 Complementation experiments with different chimeras of *B. subtilis* and *L. monocytogenes*
16 DivIVA suggest that MinJ and RacA bind to separate DivIVA domains. Fluorescence
17 microscopy of GFP-tagged RacA and MinJ corroborated this conclusion, and suggests that
18 MinJ recruitment operates via the N-terminal lipid binding domain, whereas RacA interacts
19 with the C-terminal domain. We speculate that this difference is related to the cellular
20 compartments in which MinJ and RacA are active; the cell membrane and the cytoplasm,
21 respectively.

22

INTRODUCTION

1
2 DivIVA homologues constitute a group of highly conserved cell division proteins in Gram-
3 positive bacteria. They bind to the cytosolic face of the cytoplasmic membrane and
4 accumulate at membrane regions with increased negative curvature in rod shaped bacteria (1-
5 3). Negatively curved (*i.e.* concave) membrane regions occur at the cell poles and along the
6 cytokinetic ring as soon as it starts to constrict and invaginates the cell membrane. Membrane
7 binding and curvature sensitivity appears to be an intrinsic feature of DivIVA as it was shown
8 that DivIVA of *Bacillus subtilis* also localises to curved membranes when expressed in other,
9 non-related species, including yeast cells (4). DivIVA is used as scaffold and recruits other
10 proteins that function in cell division, cell wall biosynthesis, secretion, genetic competence, or
11 chromosome segregation (5-13). The proteins that interact with DivIVA are therefore diverse
12 and comprise both trans-membrane and cytosolic proteins (14). The best characterised
13 DivIVA protein is that of *B. subtilis* for which four different interaction partners are known:
14 (i) the trans-membrane protein MinJ which acts as a molecular bridge between DivIVA and
15 the FtsZ inhibiting MinCD complex (11, 12), (ii) the DNA-binding protein RacA that is
16 required for chromosome segregation during spore formation (8, 15), (iii) the competence-
17 specific inhibitor of cell division Maf (16), and (iv) the competence regulator ComN (17).
18 Nothing is known about the molecular interaction between DivIVA and its interaction
19 partners. We set out to determine DivIVA interaction domains in more detail and focussed on
20 the binding of *B. subtilis* DivIVA with MinJ and RacA.

21 The crystal structure of *B. subtilis* DivIVA revealed a two-domain organisation; a
22 highly conserved N-terminal domain that forms a dimeric structure with a characteristic cap
23 structure and a less conserved C-terminal domain that is rich in coiled-coils but varies in
24 length among the different bacterial species (18). These domains are connected by a flexible
25 ~20 amino acid linker (Fig. 1). The N-terminal domain is required for the lipid binding of
26 DivIVA and for localization (1, 18, 19). The dimeric cap structure of this lipid binding

1 domain (LBD) exposes two phenylalanine side chains (F17, one per subunit), and the
2 insertion of these side chains into the hydrophobic core of the phospholipid bilayer is essential
3 for lipid binding (18). This membrane interaction is stabilized by auxiliary electrostatic
4 interactions between positively charged arginine and lysine residues (R18 and K15) in the
5 immediate vicinity of F17 and the negatively charged phospholipid head groups (18). The
6 crystal structure suggested that the central coiled-coil region of the C-terminal domain
7 contributes to DivIVA dimerization (Fig. 1B), and that the end of this domain (amino acids
8 130-153) forms an antiparallel four-helix bundle constituting the tetramerization domain (TD)
9 whereby two DivIVA dimers are linked together in an end-to-end orientation (18) (Fig. 1A-
10 B). The C-terminal part of DivIVA is the least conserved domain; it differs in length and can
11 contain large insertions (Fig. 1A). It was therefore speculated that this domain is responsible
12 for the interaction with other proteins (14).

13 To test whether the C-terminus of DivIVA comprises the partner interaction domain,
14 we tested C-terminally truncated variants of *B. subtilis* DivIVA for their interaction with MinJ
15 and RacA using the bacterial two-hybrid system. These experiments proved inconclusive
16 since removal of the tetramerization domain appeared to affect oligomerization. Therefore we
17 set up a complementation assay with chimeric DivIVA proteins that consist of domains from
18 *B. subtilis* and *Listeria monocytogenes* DivIVA. The latter protein localizes normally when
19 expressed in *B. subtilis* but is biologically inactive and is unable to recruit MinJ or RacA to
20 the cell division sites and cell poles. This experiment revealed that the sporulation activity and
21 the cell division activity of DivIVA can be separated. It emerged that the trans-membrane
22 protein MinJ binds to the N-terminal lipid binding domain of DivIVA, whereas the C-terminal
23 domain of DivIVA contains the binding site for the cytosolic protein RacA.

24

MATERIALS AND METHODS

Bacterial strains and growth conditions

All bacterial strains that were used in this study are listed in Table 1. Routinely, *B. subtilis* strains were cultivated in LB broth or on LB agar at 37°C. If necessary, antibiotics were added at the following concentrations: tetracycline (10 µg/ml), spectinomycin (100 µg/ml), and chloramphenicol (5 µg/ml). Other supplements were IPTG (1 mM) and xylose (0.5%). For all cloning procedures *Escherichia coli* TOP10 was used as the standard plasmid host (20).

Construction of bacterial two hybrid plasmids

In order to construct C-terminal truncations of *divIVA* for use in the bacterial two-hybrid assay, plasmid p25N-*divIVA* and pUT18-*divIVA* were used templates in a PCR with oligonucleotide 25_N_18_F as the forward and the oligonucleotides *divIVA*_11_B2H_R (Δ11), *divIVA*_19_B2H_R (Δ20), *divIVA*_21_R (Δ21), *divIVA*_26_R (Δ26), *divIVA*_34_R (Δ34) as the complementary primers (for all primer sequences see Table 2). The PCR products were KpnI digested, self-ligated and transformed to *E. coli*. The appropriate clones were identified using restriction analysis and DNA sequencing.

Construction of plasmids containing *divIVA* from *B. subtilis* and *L. monocytogenes*

For xylose-inducible expression of *B. subtilis divIVA* we constructed plasmid pSH19. This plasmid was obtained by introducing a stop codon between *divIVA* and *gfp* using plasmid pSH3 as the template and the oligonucleotides SV23/SV24 as the primers in a quick-change mutagenesis reaction. In order to express the *L. monocytogenes divIVA* gene in *B. subtilis* cells, plasmid pSH209 was constructed. This plasmid contains the complete *lmo2020* open reading frame of *L. monocytogenes* under control of the P_{xyI} promoter. It was obtained by amplification of the *L. monocytogenes divIVA* DNA fragment with the oligonucleotides

1 SHW109/SHW110 and subsequent cloning of the obtained fragment into plasmid pSG1154
2 using KpnI/XhoI. Plasmid pSH210 was constructed in the same way to allow for the
3 expression of *L. monocytogenes* DivIVA-GFP in cells of *B. subtilis*. However, for this
4 cloning, the *divIVA* DNA fragment was amplified with primers SHW109/SHW111 to fuse the
5 *divIVA* gene in frame to the *gfp* gene of the vector backbone. The A206K mutation which
6 prevents dimerization of GFP (21, 22) was introduced into the *gfp* part of plasmid pSH210
7 using quickchange mutagenesis with SHW425/SHW426 as the mutagenic primers. The
8 resulting plasmid was sequenced and named pSH354.

9

10 **Construction of *divIVA* chimeras**

11 For the construction of chimeric *divIVA* genes consisting of N-terminal parts from *L.*
12 *monocytogenes* and C-terminal parts from *B. subtilis*, a PCR based restriction free cloning
13 strategy was used (23). C-terminal fragments of *B. subtilis divIVA* gene were amplified from
14 plasmid pSH19 with SHW237 (pSH260), SHW238 (pSH261), SHW247 (pSH267), SHW265
15 (pSH272) and SHW266 (pSH278) as the respective forward and SHW184 as the reverse
16 primer in a first step. All forward primers were identical to the desired fusion sites in the *L.*
17 *monocytogenes divIVA* gene in their 5'-regions, whereas the reverse primer SHW184
18 annealed outside the *B. subtilis divIVA* gene in the pSH19 plasmid backbone. For the
19 construction of the *divIVA*^{Bs-57-Lm} chimera, a DNA fragment corresponding to the first 57
20 amino acids of the *B. subtilis divIVA* gene was amplified in a PCR with pSH19 as template
21 and SHW354 and SHW355 as the primers. All PCR products were purified using the PCR
22 purification kit from Qiagen and used as mega primers in a second PCR with plasmid pSH209
23 as template in order to fuse the N- and C-terminal fragments of *B. subtilis divIVA* to the
24 corresponding portions of the *L. monocytogenes divIVA* gene. For the construction of the
25 *divIVA*^{Bs-57-Lm} chimera (pKK13), primer SHW180 was added as a reverse primer to the PCR

1 mixture. The PCR mixtures were then DpnI digested, transformed and the correct clones were
2 identified using restriction analysis and DNA sequencing.

3 GFP was fused to all DivIVA chimeras by replacing the stop codon of the chimeric *divIVA*
4 genes by a glycine codon in a way that the *divIVA* genes was fused to the downstream *gfp*
5 ORF that was already present in these plasmids. For this purpose we used the
6 oligonucleotides SHW304/SHW305 to replace the *divIVA* stop codons in plasmids pSH260,
7 pSH261, pSH267, pSH272, and pSH278. The replacement of the *divIVA* stop codon in
8 plasmid pKK13 was performed using the primer pair SHW366/SHW367. The DNA sequence
9 of all plasmid clones was verified and the plasmids were named pSH290 (*divIVA*^{Lm-71-Bs}-
10 *gfpA206K*), pSH291 (*divIVA*^{Lm-144-Bs}-*gfpA206K*), pSH292 (*divIVA*^{Lm-130-Bs}-*gfpA206K*),
11 pSH293 (*divIVA*^{Lm-83-Bs}-*gfpA206K*), pSH294 (*divIVA*^{Lm-104-Bs}-*gfpA206K*), and pSH326
12 (*divIVA*^{Bs-57-Lm}-*gfp*). Finally, the *gfpA206K* mutation was also introduced into plasmid pSH326
13 as described above to result in plasmid pSH355.

14

15 **Construction of a *minJ-gfp* fusion**

16 In order to express a *minJ-gfp* fusion in the *divIVA* chimera strains, the *minJ-gfp* allele of
17 strain SB002 was PCR amplified using the oligonucleotides SHW342/SHW343, cut
18 BamHI/SalI, ligated to pAPNC213cat digested with the same enzymes, and the resulting
19 plasmid was named pSH316 after DNA sequencing. However, there was only marginal MinJ-
20 GFP fluorescence, when pSH316 was inserted into the *B. subtilis* chromosome under inducing
21 conditions (strain BSN308, data not shown). Therefore, plasmid pSH317 was constructed in
22 which the *lacI* gene of pSH316 was deleted by PCR using the primer pair SHW349/SHW350
23 in order to enhance the fluorescence signal. MinJ-GFP fluorescence was still not sufficient
24 with this allele (strain BSN317, data not shown), so the promoter region of the *B. subtilis*
25 *divIVA* gene including the ribosomal binding site was amplified with primers SV98/SHW356,
26 cut with KpnI and XhoI, and ligated to pSH317 which had been cut with the same enzymes.

1 Two clones were isolated that contained a *divIVA* promoter insert of the right size but DNA
2 sequencing revealed single mutations in the RBS ($P_{divIVA1}$ on pSH320). In order to correct this,
3 quick-change mutagenesis with primers SHW357/SHW358 was employed on pSH320 and
4 several plasmid clones were isolated and transformed to *B. subtilis*. From these
5 transformations, only three plasmid clones conferred the typical fluorescence pattern of MinJ-
6 GFP on cells of *B. subtilis*. When sequenced, one of these clones had a corrected RBS but
7 also an unintended G deletion between the RBS and the MinJ-GFP start codon ($P_{divIVA3}$). This
8 clone was named pSH328 and used for all further studies.

9

10 **Construction of point mutations and C-terminal truncations in *divIVA***

11 For the construction of plasmid pINC12 encoding the *divIVAR131A* gene under control of the
12 P_{spac} promoter, we made use of plasmid pINC3 which already contained the *divIVAR131A-gfp*
13 allele. pINC3 was originally obtained by quick change mutagenesis using the mutagenesis
14 primers R131A_fw/R131A_rev on plasmid pDG9. *divIVAR131A* of pINC3 was then
15 amplified using the primers SV123/SV81, the resulting PCR fragment was cut with
16 BamHI/SalI, and ligated to the BamHI/SalI cut vector backbone of plasmid pAPNC213. The
17 DNA sequence of one clone was verified and this clone was named pINC12. The R102K,
18 R102E, and $\Delta C34$ mutations were introduced into plasmid pSH2 by quick-change
19 mutagenesis using the oligonucleotides SHW378/SHW379 (pSH330), SHW380/SHW381
20 (pSH331), and SHW386/SHW387 (pSH334), respectively. In order to exchange the *spc*
21 marker by a *cat* cassette in these plasmids, the KpnI/SacI P_{spac} -*divIVA* fragments of pSH2,
22 pSH330, pSH331, and pSH334 were then sub-cloned into the KpnI/SacI cut backbone of
23 pAPNC213cat in a second step. The resulting plasmids were sequenced and named pSH335
24 (wt), pSH336 (R102K), pSH337 (R102E), and pSH340 ($\Delta C34$).

25

1 **Strain construction**

2 Plasmids designed for the expression of *divIVA* alleles in *B. subtilis* were inserted into the
3 *amyE* gene of *B. subtilis* 168 and amylase negative transformants were selected based on
4 iodine staining of starch containing agar plates. Alternatively, the *aprE* locus was also used
5 for chromosomal integrations. Insertions at *aprE* were generally confirmed by PCR.
6 Combinations of alleles were generated by transformation (24).

7

8 **Bacterial two-hybrid analysis**

9 In order to investigate the interaction of the DivIVA and C-terminally truncated DivIVA
10 proteins with MinJ and RacA, the bacterial two-hybrid system was used (25). Plasmids
11 encoding *divIVA* alleles fused to the T18- or the T25- fragment of the *Bordetella pertussis*
12 adenylate cyclase were co-transformed in *E. coli* BTH101 along with plasmids encoding T25-
13 and T18-fusions to RacA and MinJ. Transformants were selected on nutrient agar plates
14 containing ampicillin (100 µg/ml), kanamycin (50 µg/ml), X-Gal (0.004%) and IPTG (0.1
15 mM) and photographs were taken after 40 h of growth at 30°C.

16

17 **Microscopic techniques**

18 For microscopy of bacterial cells, a small volume (0.3 µl) of an exponentially growing culture
19 was mounted on a microscope slide covered with a thin film of 1.5% agarose (dissolved in
20 distilled water). Membranes were stained using FM5-95. Images were taken with a Nikon
21 Eclipse Ti microscope coupled to a Nikon DS-MBWc CCD camera and processed using the
22 NIS elements AR software package (Nikon).

23

24 **Sporulation assays**

25 *B. subtilis* strains were streaked on Schaeffer's sporulation agar (26) containing 0.5% xylose
26 or 1 mM IPTG and incubated for up to seven days at 37°C until lysis of the translucent

1 sporulation-deficient strains could be comfortably discriminated from the optically dense
2 appearance of sporulation-proficient strains. Plates were photographed against a black
3 background.

4

5 **Isolation of cellular proteins, PAGE techniques and Western blotting**

6 Exponentially growing cells of *B. subtilis* were harvested by centrifugation (13.000 rpm for 1
7 min in an Eppendorf 5415R table top centrifuge) and the cell pellet was washed once in ZAP
8 buffer (10 mM Tris-HCl pH 7.5, 200 mM NaCl). Cells were disrupted by sonication in ZAP
9 buffer containing 1 mM PMSF and cell debris was pelleted in another centrifuge run.
10 Aliquots of the resulting supernatant were either separated by SDS PAGE or by blue native
11 PAGE which was performed using NativePAGE™ Novex ® 4-16% Bis-Tris gels (Invitrogen)
12 and carried out according to the instructions given by the manufacturer. Subsequently, gels
13 were blotted onto a polyvinylidene difluoride (PVDF) membrane employing a semi-dry
14 electroblotting unit. Proteins of interest were visualised using polyclonal rabbit antisera
15 recognizing DivIVA (5) or GFP (lab stock) as the primary antibodies and an anti-rabbit
16 immunoglobulin G conjugated to horseradish peroxidase as the secondary one. The ECL
17 chemiluminescence detection kit (Thermo Scientific) was then used for the detection of the
18 peroxidase conjugates on the PVDF membranes.

19

20

RESULTS

C-terminal DivIVA truncations interfere with MinJ and RacA binding

The tetramerization domain of *B. subtilis* DivIVA is followed by 11 non-conserved amino acid residues. The atomic structure of this C-terminal stretch could not be solved using crystallography, suggesting that it is a flexible tail. To determine whether this C-terminal tail is involved in the binding of MinJ and/or RacA, we made use of the bacterial two-hybrid assay and cloned two DivIVA truncations in this system: DivIVA Δ 11 lacking the last 11 C-terminal amino acids, and DivIVA Δ 20 which lacks the last 20 C-terminal amino acids including a part of the tetramerization domain (Table 3). Both truncations were still able to interact with full-length DivIVA, indicating that both mutants are expressed normally and can form dimers (Table 3, a colored image of the bacterial two-hybrid plate is available in Fig. S1). MinJ interacted strongly with full length DivIVA and with both DivIVA truncations in the bacterial two-hybrid assay, whereas RacA showed a weak interaction with full length DivIVA that was abolished when the last 11 amino acids of DivIVA were removed (Table 3, Fig. S1). It seems that the RacA-DivIVA interaction depends on the 11 C-terminal amino acids of DivIVA, whereas the MinJ contact site is located more to the N-terminus of DivIVA. To test this, additional DivIVA truncations were constructed: DivIVA Δ 21, DivIVA Δ 26, and DivIVA Δ 34, which successively removed the complete tetramerization domain. The latter two truncations, DivIVA Δ 26 and DivIVA Δ 34, were severely impaired in their ability to interact with MinJ (Table 3, Fig. S1), suggesting that the tetramerization domain contains residues required for MinJ binding.

Importance of the tetramerization domain for DivIVA activity

The bacterial two-hybrid assay also revealed a weakened interaction of the DivIVA Δ 26 (corresponding to DivIVA amino acids 1-138) and DivIVA Δ 34 (1-130) truncations with full-length DivIVA whereas DivIVA Δ 21 (1-143) still behaved normal (Table 3, Fig. S1). So far

1 there is no biochemical corroboration that amino acids 130-143 are involved in
2 tetramerization *in vivo*. Own preliminary alanine mutagenesis experiments in this region
3 identified R131 as an essential residue for DivIVA activity (Fig. S3 A-C) suggesting a special
4 importance of this region for DivIVA function. Thus, DivIVA Δ C34 was expressed in a
5 Δ *divIVA* mutant (strain BSN360) and phenotypic analysis of this strain clearly demonstrated
6 the inability of the *divIVA* Δ C34 allele to complement the cell division and the sporulation
7 phenotype of the Δ *divIVA* mutation (Fig. 2A-B) even though DivIVA Δ C34 was clearly
8 expressed (Fig. 2C, upper panel). Blue native PAGE of strain BSN356 expressing wild-type
9 DivIVA showed that DivIVA exists in two different oligomeric states since two signals of
10 different molecular weight were detected by the DivIVA antiserum (Fig. 2C, bottom panel).
11 The molecular weight was calculated to be 159 \pm 8 kDa for the upper and 41 \pm 13 kDa for the
12 lower signal in the wild type cell extract. Given the molecular weight of *Bs* DivIVA (19.34
13 kDa), these molecular weights correspond to an octamer and a dimer, respectively. Blue
14 native PAGE of strain BSN360 revealed the existence of a dimer signal (Fig. 2C, bottom
15 panel). Previous gel filtration analyses have indicated that purified DivIVA forms octamers
16 and higher-order structures (18, 27). Therefore it seems plausible that the region beyond
17 residue 130 indeed contains the tetramerization domain, and that tetramerization is a
18 prerequisite step for octamerization.

19

20 **Domain swapping to identify DivIVA interaction domains**

21 It is possible that C-terminal truncations used in the bacterial two-hybrid system result in
22 misfolded and/or instable DivIVA variants. This complicates the interpretation of the bacterial
23 two-hybrid data. Because of this we changed tactics and explored the possibility to swap
24 domains between *B. subtilis* DivIVA and the closely homologous DivIVA from *L.*
25 *monocytogenes*. In a previous study, we have shown that *L. monocytogenes* DivIVA displays
26 the same localization pattern as *B. subtilis* DivIVA, and is involved in SecA2-dependent

1 protein secretion (10). *L. monocytogenes* does not sporulate and does not contain a RacA
2 homologue. It is also unlikely that *L. monocytogenes* DivIVA interacts with MinJ since
3 deletion of the *divIVA* gene does not result in a mini-cell phenotype in *L. monocytogenes*,
4 indicating that the listerial division site control system is DivIVA-independent (10). This
5 would enable us to separate the DivIVA domains required for localization and for RacA and
6 MinJ interaction. First it was necessary to confirm that *L. monocytogenes* DivIVA is normally
7 localized when expressed in *B. subtilis*. Indeed, *L. monocytogenes* DivIVA fused to GFP and
8 expressed in a *divIVA* knock-out background (strain BSN373) shows a localization pattern
9 that is similar to that of *Bs* DivIVA (Fig. 3) even though *Lm* DivIVA predominantly exists as
10 a dimer and just to a minor extent in an oligomeric form when expressed in *B. subtilis* (Fig.
11 S2). More importantly however, *Lm* DivIVA does not complement the cell division and
12 sporulation defects of a *B. subtilis* $\Delta divIVA$ mutant (strain BSN238, Fig. 5A-B). Thus, *Lm*
13 DivIVA seems unable to bind MinJ and RacA, and is therefore well suited for domain
14 swapping.

15 The most prominent difference between *Lm* and *Bs* DivIVA is found in the C-terminal
16 tail (Fig. 4A), which is 11 amino acids longer in the *L. monocytogenes* protein, and which has
17 been shown to be important for binding RacA according to the bacterial two-hybrid data. To
18 test this, a DivIVA chimera was constructed by replacing the last 32 amino acids of *Lm*
19 DivIVA with the last 21 amino acids of *Bs* DivIVA (*Lm*-144-*Bs*), so that the C-terminal tails
20 were exchanged between both proteins whereas the core tetramerization domain (130-143)
21 was left intact (Fig. 4B). Expression of this chimera in a *B. subtilis* $\Delta divIVA$ background
22 (strain BSN274) did neither restore cell division nor sporulation (Fig. 5A,B). Western blotting
23 showed that *Lm*-144-*Bs* DivIVA was stably expressed and not degraded (Fig. 4C). The
24 chimeric protein localized normally, as a GFP fusion indicated (strain BSN295, Fig. S4) and
25 formed a stable oligomer (Fig. S2), suggesting that the last 21 amino acids of *Bs* DivIVA
26 alone are insufficient for binding of MinJ or RacA.

1 **Systematic domain swapping**

2 Since RacA binding seems to require a larger part of *Bs* DivIVA we constructed a set of
3 chimeric DivIVA proteins in which the fusion point between the N-terminal *L.*
4 *monocytogenes* and the C-terminal *B. subtilis* parts was shifted from the tail region towards
5 the N-terminus of the C-terminal domain in a stepwise fashion, as schematically indicated in
6 Fig. 4B. Position 130 exchanged the complete C-terminus beginning from the TD, positions
7 104 and 83 mark the beginning of short stretches in the coiled coil region at which both
8 proteins differ at three to four consecutive amino acid positions, whereas the domain swap at
9 position 71 exchanged the complete C-terminal domain behind the flexible linker (Fig. 4A-B).
10 Stability and oligomerization of the chimeras was checked by Western blotting indicating that
11 all the chimeric DivIVA proteins were expressed at comparable levels (Fig. 4C) and were
12 oligomeric (Fig. S2). Expression of these chimeras in the *B. subtilis* $\Delta divIVA$ background did
13 not restore normal vegetative cell division (Fig. 5A) suggesting that they were unable to
14 recruit MinJ. Of the different chimera, only the *Lm-104-Bs* DivIVA chimera was able to
15 restore spore formation. To confirm that the *Lm-104-Bs* DivIVA chimera was indeed able to
16 recruit RacA and not MinJ, the chimera was expressed in $\Delta divIVA$ mutant strains either
17 containing the GFP-RacA or the MinJ-GFP reporter. As shown in Fig. 6A-B, the *Lm-104-Bs*
18 DivIVA chimera can recruit RacA but not MinJ. In conclusion, the RacA interaction domain
19 resides in the last 60 amino acids of DivIVA and requires residues in the coiled-coiled region
20 beyond amino acid 104.

21 It is surprising that larger replacements of the C-terminus (as in *Lm-71-Bs* and *Lm-83-*
22 *Bs*) are again unable to restore sporulation. A possibility is that these chimeras do not localize
23 properly anymore. To test this, we expressed C-terminal GFP fusions to the chimeric DivIVA
24 constructs, and analysed their localization in *B. subtilis* $\Delta divIVA$ cells. Expression of all
25 DivIVA-GFP proteins gave rise to polar and septal fluorescence signals, however, to different
26 degrees (Fig. S4A). While DivIVA^{*Lm-144-Bs*}-GFP and DivIVA^{*Lm-130-Bs*}-GFP clearly

1 accumulated at the division septa, septal fluorescence signals of DivIVA^{Lm-104-Bs}-GFP,
2 DivIVA^{Lm-83-Bs}-GFP, and DivIVA^{Lm-71-Bs}-GFP were less intense but still visible (Fig. S4A).
3 This suggests that all DivIVA chimeras are functional in terms of lipid binding and membrane
4 curvature sensing.

5

6 **The lipid binding domain recruits MinJ**

7 As none of the chimeras was able to complement the cell division phenotype, it may be that
8 regions in the N-terminal domain are critical for the interaction of *Bs* DivIVA with MinJ. To
9 test this, we fused the N-terminal 57 amino acids of *B. subtilis* DivIVA spanning the entire
10 lipid binding domain to the complete C-terminal domain of *L. monocytogenes* DivIVA (Fig.
11 4B). When this DivIVA chimera was expressed in a $\Delta divIVA$ background (strain BSN321),
12 short cells and no mini-cells were observed (Fig. 5A), indicating that the *Bs-57-Lm* DivIVA
13 protein recruits MinJ. The localization as well as oligomerization of this chimera is
14 comparable to wild type DivIVA (Fig. S4 and Fig. S2, respectively) and indeed restores
15 normal septal and polar localization of GFP-MinJ (Fig. 6A). Strikingly, sporulation was still
16 defective in strain BSN321 (Fig. 5B) and the *Bs-57-Lm* chimera is unable to recruit RacA
17 (Fig. 6B). In conclusion, the lipid binding N-terminal domain of DivIVA contains the MinJ
18 binding site whereas the C-terminal coiled-coil domain contains the binding site for RacA.

19

DISCUSSION

1
2 Here we show that two of the DivIVA interaction partners from *B. subtilis*, MinJ and RacA,
3 bind to mutually exclusive surface regions of DivIVA. This was concluded from
4 complementation assays with DivIVA chimeras constructed from *B. subtilis* and *L.*
5 *monocytogenes* DivIVA. Analysis of a set of such DivIVA chimeras in complementation
6 experiments surprisingly revealed that the N-terminal lipid binding domain provides the MinJ
7 interaction module whereas RacA binds to the C-terminal domain of DivIVA. This was
8 unexpected since it was assumed that the C-terminal domain would constitute the protein
9 recruitment module for both proteins, with the LBD being important only for dimerization
10 and lipid binding. However, a dual function of the lipid binding domain is in good agreement
11 with the two-domain nature of DivIVA proteins. The lipid binding domain is in close contact
12 to the cytoplasmic membrane and even partially inserts into it, which makes it a good
13 candidate for interacting with trans-membrane proteins like MinJ. Since most sequence
14 differences between the LBDs of *Bs* and *Lm* DivIVA cluster between residues E28 and I57
15 (Fig. 4A), this region most likely represents the MinJ binding surface of DivIVA. Support for
16 this assumption comes from the observation that a replacement of region 1-16 of
17 *Corynebacterium glutamicum* DivIVA by the corresponding region from *Bs* DivIVA was
18 without effect (19). Lipid binding of DivIVA via its N-terminal domain would in turn leave
19 the C-terminus free to reach into the cytoplasm. Fitting with this, our experiments indicated
20 that the C-terminal domain is the interaction module for RacA which is a soluble cytoplasmic
21 protein. It was recently reported that the interaction of *C. glutamicum* ParB, which is a
22 chromosome-binding protein like RacA, to its cognate DivIVA requires central regions of the
23 C-terminal domain as well (9). Our results thus confirm earlier speculations that the
24 sporulation and the division functions of DivIVA can be separated. This had been concluded
25 from the observation that a *divIVAN99D* mutation severely affected sporulation but not
26 division (28). Another classical *divIVA* point mutation is the *divIVA1* mutation in which the

1 alanine at position 78 is substituted by a threonine. This mutation causes a *div⁻ spo⁻* phenotype
2 (29) even though it lies outside the RacA and MinJ binding regions. Neither expression nor
3 oligomerization of DivIVA is impaired by this mutation (30). Thus, the A78T exchange might
4 possibly affect subcellular localisation of DivIVA or induce structural changes in the protein
5 that reduce its activity but do not influence formation of oligomers.

6 The question that we cannot answer conclusively is: Why do the two chimeras with the more
7 N-terminally located fusion points (*Lm-83-Bs* and *Lm-71-Bs*) not behave similar to the *Lm-*
8 *104-Bs* DivIVA protein? Initially, this conflicted with the idea that C-terminal domain is the
9 protein recruitment module for RacA, since longer C-terminal exchanges than in *Lm-104-Bs*
10 should result at least in the same degree of complementation activity. We do not think that
11 this is explained by misfolding of the respective chimeric proteins since they still oligomerize
12 (Fig. S2) and because GFP-tagged versions of these chimeras still localised to the septum in
13 the same degree as the *Lm-104-Bs* GFP fusion protein (Fig. S4A) and therefore appeared to be
14 folded properly. Moreover, a strain expressing an *Lm-57-Bs* DivIVA protein showed the same
15 sporulation defect as strains expressing *Lm-83-Bs* and *Lm-71-Bs* DivIVA chimeras (data not
16 shown). Possibly, longer C-terminal exchanges do not function in the context of an unrelated
17 lipid binding domain. With regard to this issue, the fact that the arginine 102 residue of *Bs*
18 DivIVA is phosphorylated might be of special interest here (31). This phosphorylation could
19 be critical for RacA recruitment and may add an extra dimension of activity control on the
20 different DivIVA chimeras. Therefore, we constructed a phospho-ablative (R102K) and a
21 phospho-mimetic (R102E) mutant allele of *divIVA* and tested their activity in our
22 complementation system. Both of these mutations cause a *div⁺ spo⁻* phenotype (Fig. S5).
23 Hence, arginine 102 might indeed have a crucial function in RacA binding but it is not
24 relevant for the interaction with MinJ. Phosphorylations at the C-terminal domains are well
25 described for DivIVA from *Mycobacterium tuberculosis* (named Wag31 in mycobacteria) and
26 *Streptococcus pneumoniae* even though they both occurred at threonine side chains (T73 and

1 T201, respectively). Phenotypic analysis of phospho-mimetic and phospho-ablative *divIVA*
2 mutant strains in these organisms also revealed that these phosphorylations are indeed
3 involved in cell shape control (32, 33). In the future it will be interesting to address the
4 regulatory impact of such phosphorylations for DivIVA binding partner recruitment.

5

6

ACKNOWLEDGEMENTS

7 The authors thank Ling Juan Wu (Newcastle University) for the kind gift of the *gfp-racA*
8 strain and Henrik Strahl (Newcastle University) for sharing plasmid pAPNC213cat. This
9 work was financially supported by a DAAD fellowship to K.G.K, a DFG grant (BR-2915/2-1)
10 to M.B. and a Wellcome Trust Research Career Development Fellowship as well as a
11 Biological Sciences Research Council Grant to L.W.H.

12

REFERENCES

1. **Lenarcic R, Halbedel S, Visser L, Shaw M, Wu LJ, Errington J, Marenduzzo D, Hamoen LW.** 2009. Localisation of DivIVA by targeting to negatively curved membranes. *EMBO J.* **28**:2272-2282.
2. **Ramamurthi KS, Losick R.** 2009. Negative membrane curvature as a cue for subcellular localization of a bacterial protein. *Proc. Natl. Acad. Sci. U S A* **106**:13541-13545.
3. **Eswaramoorthy P, Erb ML, Gregory JA, Silverman J, Pogliano K, Pogliano J, Ramamurthi KS.** 2011. Cellular architecture mediates DivIVA ultrastructure and regulates Min activity in *Bacillus subtilis*. *MBio* **2**: e00257-11. 10.1128/mBio.00257-11.
4. **Edwards DH, Thomaidis HB, Errington J.** 2000. Promiscuous targeting of *Bacillus subtilis* cell division protein DivIVA to division sites in *Escherichia coli* and fission yeast. *EMBO J.* **19**:2719-2727.
5. **Marston AL, Thomaidis HB, Edwards DH, Sharpe ME, Errington J.** 1998. Polar localization of the MinD protein of *Bacillus subtilis* and its role in selection of the mid-cell division site. *Genes Dev.* **12**:3419-3430.
6. **Letek M, Ordonez E, Vaquera J, Margolin W, Flärdh K, Mateos LM, Gil JA.** 2008. DivIVA is required for polar growth in the MreB-lacking rod-shaped actinomycete *Corynebacterium glutamicum*. *J. Bacteriol.* **190**:3283-3292.
7. **Xu H, Chater KF, Deng Z, Tao M.** 2008. A cellulose synthase-like protein involved in hyphal tip growth and morphological differentiation in *Streptomyces*. *J. Bacteriol.* **190**:4971-4978.
8. **Wu LJ, Errington J.** 2003. RacA and the Soj-Spo0J system combine to effect polar chromosome segregation in sporulating *Bacillus subtilis*. *Mol. Microbiol.* **49**:1463-1475.
9. **Donovan C, Sieger B, Krämer R, Bramkamp M.** 2012. A synthetic *Escherichia coli* system identifies a conserved origin tethering factor in *Actinobacteria*. *Mol. Microbiol.* **84**:105-116.
10. **Halbedel S, Hahn B, Daniel RA, Flieger A.** 2012. DivIVA affects secretion of virulence-related autolysins in *Listeria monocytogenes*. *Mol. Microbiol.* **83**:821-839.
11. **Bramkamp M, Emmins R, Weston L, Donovan C, Daniel RA, Errington J.** 2008. A novel component of the division-site selection system of *Bacillus subtilis* and a new mode of action for the division inhibitor MinCD. *Mol. Microbiol.* **70**:1556-1569.
12. **Patrick JE, Kearns DB.** 2008. MinJ (YvjD) is a topological determinant of cell division in *Bacillus subtilis*. *Mol. Microbiol.* **70**:1166-1179.
13. **Flärdh K.** 2003. Essential role of DivIVA in polar growth and morphogenesis in *Streptomyces coelicolor* A3(2). *Mol. Microbiol.* **49**:1523-1536.
14. **Kaval KG, Halbedel S.** 2012. Architecturally the same, but playing a different game: The diverse species-specific roles of DivIVA proteins. *Virulence* **3**:406-407.
15. **Ben-Yehuda S, Rudner DZ, Losick R.** 2003. RacA, a bacterial protein that anchors chromosomes to the cell poles. *Science* **299**:532-536.
16. **Briley K, Jr., Prepiak P, Dias MJ, Hahn J, Dubnau D.** 2011. Maf acts downstream of ComGA to arrest cell division in competent cells of *B. subtilis*. *Mol. Microbiol.* **81**:23-39.
17. **Dos Santos VT, Bisson-Filho AW, Gueiros-Filho FJ.** 2012. DivIVA-mediated polar localization of ComN, a post-transcriptional regulator of *B. subtilis*. *J. Bacteriol.* **194**:3661-3669.

- 1 18. **Oliva MA, Halbedel S, Freund SM, Dutow P, Leonard TA, Veprintsev DB,**
2 **Hamoen LW, Löwe J.** 2010. Features critical for membrane binding revealed by
3 DivIVA crystal structure. *EMBO J.* **29**:1988-2001.
- 4 19. **Letek M, Fiuza M, Ordonez E, Villadangos AF, Flärdh K, Mateos LM, Gil JA.**
5 2009. DivIVA uses an N-terminal conserved region and two coiled-coil domains to
6 localize and sustain the polar growth in *Corynebacterium glutamicum*. *FEMS*
7 *Microbiol. Lett.* **297**:110-116.
- 8 20. **Sambrook J, Fritsch EF, Maniatis T.** 1989. Molecular cloning: a laboratory manual,
9 2nd ed. Cold Spring Harbor Laboratory Press, Cold Spring Harbor, N.Y.
- 10 21. **Zacharias DA, Violin JD, Newton AC, Tsien RY.** 2002. Partitioning of lipid-
11 modified monomeric GFPs into membrane microdomains of live cells. *Science*
12 **296**:913-916.
- 13 22. **Landgraf D, Okumus B, Chien P, Baker TA, Paulsson J.** 2012. Segregation of
14 molecules at cell division reveals native protein localization. *Nat. Methods* **9**:480-482.
- 15 23. **van den Ent F, Löwe J.** 2006. RF cloning: a restriction-free method for inserting
16 target genes into plasmids. *J. Biochem. Biophys. Methods* **67**:67-74.
- 17 24. **Hamoen LW, Smits WK, de Jong A, Holsappel S, Kuipers OP.** 2002. Improving
18 the predictive value of the competence transcription factor (ComK) binding site in
19 *Bacillus subtilis* using a genomic approach. *Nucleic Acids Res.* **30**:5517-5528.
- 20 25. **Karimova G, Pidoux J, Ullmann A, Ladant D.** 1998. A bacterial two-hybrid system
21 based on a reconstituted signal transduction pathway. *Proc. Natl. Acad. Sci. U S A*
22 **95**:5752-5756.
- 23 26. **Harwood CR, Coxon RD, Hancock IC.** 1990. Molecular biological methods for
24 *Bacillus*. John Wiley and Sons, Chichester.
- 25 27. **Stahlberg H, Kutejova E, Muchová K, Gregorini M, Lustig A, Müller SA,**
26 **Olivieri V, Engel A, Wilkinson AJ, Barák I.** 2004. Oligomeric structure of the
27 *Bacillus subtilis* cell division protein DivIVA determined by transmission electron
28 microscopy. *Mol. Microbiol.* **52**:1281-1290.
- 29 28. **Thomaides HB, Freeman M, El Karoui M, Errington J.** 2001. Division site
30 selection protein DivIVA of *Bacillus subtilis* has a second distinct function in
31 chromosome segregation during sporulation. *Genes Dev.* **15**:1662-1673.
- 32 29. **Cha JH, Stewart GC.** 1997. The *divIVA* minicell locus of *Bacillus subtilis*. *J.*
33 *Bacteriol.* **179**:1671-1683.
- 34 30. **Muchová K, Kutejova E, Scott DJ, Brannigan JA, Lewis RJ, Wilkinson AJ,**
35 **Barák I.** 2002. Oligomerization of the *Bacillus subtilis* division protein DivIVA.
36 *Microbiology* **148**:807-813.
- 37 31. **Elsholz AK, Turgay K, Michalik S, Hessling B, Gronau K, Oertel D, Mäder U,**
38 **Bernhardt J, Becher D, Hecker M, Gerth U.** 2012. Global impact of protein
39 arginine phosphorylation on the physiology of *Bacillus subtilis*. *Proc. Natl. Acad. Sci.*
40 *U S A* **109**:7451-7456.
- 41 32. **Kang CM, Abbott DW, Park ST, Dascher CC, Cantley LC, Husson RN.** 2005.
42 The *Mycobacterium tuberculosis* serine/threonine kinases PknA and PknB: substrate
43 identification and regulation of cell shape. *Genes Dev.* **19**:1692-1704.
- 44 33. **Fleurie A, Cluzel C, Guiral S, Freton C, Galisson F, Zanella-Cleon I, Di Guilmi**
45 **AM, Grangeasse C.** 2012. Mutational dissection of the S/T-kinase StkP reveals
46 crucial roles in cell division of *Streptococcus pneumoniae*. *Mol. Microbiol.* **83**:746-
47 758.
- 48 34. **Barák I, Prepiak P, Schmeisser F.** 1998. MinCD proteins control the septation
49 process during sporulation of *Bacillus subtilis*. *J. Bacteriol.* **180**:5327-5333.

- 1 35. **Morimoto T, Loh PC, Hirai T, Asai K, Kobayashi K, Moriya S, Ogasawara N.**
2 2002. Six GTP-binding proteins of the Era/Obg family are essential for cell growth in
3 *Bacillus subtilis*. *Microbiology* **148**:3539-3552.
- 4 36. **Lewis PJ, Marston AL.** 1999. GFP vectors for controlled expression and dual
5 labelling of protein fusions in *Bacillus subtilis*. *Gene* **227**:101-110.
- 6 37. **van Baarle S, Bramkamp M.** 2010. The MinCDJ system in *Bacillus subtilis* prevents
7 minicell formation by promoting divisome disassembly. *PLoS One* **5**:e9850.
8
9

FIGURE LEGENDS

1
2
3 **Figure 1:** Domain arrangement of *B. subtilis* DivIVA. (A) Schematic sequence alignment of
4 DivIVA proteins of different phylogenetic origin. Abbreviations above the alignment label the
5 individual protein regions: LBD – lipid binding domain, CTD – C-terminal domain, TD –
6 tetramerization domain, tail – C-terminal tail region. Amino acid numbering is according to *B.*
7 *subtilis* DivIVA. (B) Model of the crystal structure of the full-length *B. subtilis* DivIVA
8 tetramer which has been assembled from the individual crystal structures of the N- and the C-
9 terminal domains (18). Crystallographic data for the linker between both domains are not
10 available (residues 53-70). Amino acid positions at the beginning and the end of the lipid
11 binding domain as well as the C-terminal domain are indicated for one molecule. Truncation
12 sites of DivIVA Δ C26 and DivIVA Δ C34 at positions 138 and 130, respectively, are also
13 shown (compare Table 3).

14
15 **Figure 2:** Complementation activity and oligomerization of a C-terminally truncated DivIVA
16 protein devoid of the tetramerization domain. (A) Phase contrast micrographs showing
17 cellular morphology of strain BSN360 expressing the DivIVA Δ C34 protein. Cultures of strain
18 168 (wt), strain 4041 (Δ *divIVA*) and the complemented Δ *divIVA* mutant strain BSN356
19 (+*divIVA*) were included for control. Cells were cultivated in LB broth (containing 1 mM
20 IPTG where necessary) to mid-logarithmic growth phase at 37°C before images were taken.
21 Scale bar is 5 μ m. (B) Sporulation of the same set of strains on Schaeffers sporulation agar
22 containing 1 mM IPTG. Cells were kept for 3 days at 37°C until lysis of the *spo*⁻ strains
23 became apparent. (C) Western blots after SDS-PAGE and blue native PAGE to analyse
24 expression and oligomerization of DivIVA Δ C34. Strains BSN356 (+*divIVA*) and BSN360
25 (+ Δ C34) were cultivated as described above and cellular protein extracts were subjected to
26 SDS-PAGE (upper panel) or blue native PAGE (bottom panel) and subsequent Western
27 blotting. DivIVA was detected using the polyclonal anti-DivIVA antiserum. The

1 NativeMarkTM standard (Invitrogen) was used as a molecular weight marker for blue native
2 PAGE.

3

4 **Figure 3:** Localization of *L. monocytogenes* DivIVA-GFP in a *B. subtilis* $\Delta divIVA$
5 background. Strain BSN373 (expressing *Lm* DivIVA-GFPA206K) was grown in LB
6 supplemented with 0.5% xylose. The localization pattern of *Lm* DivIVA-GFP was analysed
7 by epifluorescence microscopy (right image), and for orientation, a FM5-95 stained image
8 (left panel) was taken in parallel. Scale bar is 5 μ m, several septal DivIVA-GFP signals are
9 indicated by arrows.

10

11 **Figure 4:** Expression of *Lm/Bs* DivIVA chimeras in *B. subtilis*. (A) Sequence alignment of
12 the DivIVA proteins from *B. subtilis* (*Bs*) and *L. monocytogenes* (*Lm*). Identical amino acid
13 positions are indicated by a black, similar amino acid positions by a grey background. The
14 exchange sites in the different chimeras are labelled by asterisks. (B) Schematic illustration of
15 the domain organisation of the *Bs* and *Lm* DivIVA proteins and composition of all *Lm/Bs*
16 DivIVA chimeras. Abbreviations are as in Fig. 1A. The complementation activity of the
17 DivIVA chimeras in the complementation assays for division (*div*) and sporulation (*spo*) is
18 indicated in the table on the right side (compare Fig. 5). (C) Western blot showing expression
19 of the DivIVA chimeras in a *B. subtilis* $\Delta divIVA$ background. The wild type strain 168 and the
20 $\Delta divIVA$ mutant (4041) as well as strains expressing *B. subtilis* *divIVA* (BSN51) or *L.*
21 *monocytogenes* *divIVA* (BSN238) were included as controls and the DivIVA proteins were
22 detected with an antiserum that had been raised against *B. subtilis* DivIVA (5).

23

24 **Figure 5:** Complementation activity of *Lm/Bs* DivIVA chimeras in the *B. subtilis* $\Delta divIVA$
25 background. (A) Phase contrast micrographs showing the ability of the tested *Lm/Bs* DivIVA
26 chimeras to complement the filamentous $\Delta divIVA$ phenotype. Cells were cultivated in LB

1 broth containing 0.5% xylose until mid-log growth phase at 37°C before cell morphology was
2 assessed microscopically. Scale bar is 5 μm. (B) Sporulation plate assay to test the activity of
3 the *Lm/Bs* DivIVA chimeras to complement the sporulation defect of the *B. subtilis* $\Delta divIVA$
4 mutant. Strains expressing the DivIVA chimeras were streaked on Schaeffer's sporulation
5 agar containing 0.5% xylose and kept at 37°C until lysis of non-sporulating strains was
6 comfortably distinguishable from the brownish *spo*⁺ strains. The wild type, the $\Delta divIVA$
7 mutant and strains complemented either with the *B. subtilis* (BSN51) or the *L. monocytogenes*
8 *divIVA* gene (BSN238) were used as controls. 1 – strain 168 (wt), 2 – strain 4041 ($\Delta divIVA$), 3
9 – strain BSN51 (+*Bs divIVA*), 4 – strain BSN238 (+*Lm divIVA*), 5 – strain BSN274 (+*Lm*-
10 144-*Bs divIVA*), 6 – strain BSN278 (+*Lm*-130-*Bs divIVA*), 7 – strain BSN288 (+*Lm*-104-*Bs*
11 *divIVA*), 8 – strain BSN287 (+*Lm*-83-*Bs divIVA*), 9 – strain BSN316 (+*Lm*-71-*Bs divIVA*), 10
12 – strain BSN321 (+*Bs*-57-*Lm divIVA*). Please note that sporulation of strain strain BSN288
13 (+*Lm*-104-*Bs divIVA*) did not reach wild type level. This might be explained by the lack of
14 MinCD activity in this strain which is required for full sporulation (34).

15

16 **Figure 6:** Localization of MinJ and RacA in *B. subtilis* strains expressing selected *Lm/Bs*
17 *divIVA* chimeras. (A) Fluorescence micrographs showing the subcellular localization of MinJ-
18 GFP in *Lm/Bs divIVA* chimera strains during mid-logarithmic growth in LB broth
19 supplemented with 0.5% xylose at 37°C (top row). MinJ-GFP was imaged in strains
20 expressing *Lm*-104-*Bs* DivIVA (strain BSN336) and the *Bs*-57-*Lm* DivIVA chimera (strain
21 BSN338). For control, MinJ-GFP was also visualised in $\Delta divIVA$ strains which express *Bs*
22 *divIVA* (strain BSN334) or *Lm divIVA* (strain BSN335). Phase contrast images were included
23 for better orientation (bottom row). (B) Localization of RacA in *B. subtilis* strains expressing
24 the same *Lm/Bs divIVA* chimeras as in panel A. Fluorescence images were obtained on cells
25 during growth in LB broth containing 0.5% xylose at 37°C (top row). GFP-RacA was
26 visualized in strains expressing the *Lm*-104-*Bs* DivIVA (strain BSN342) and *Bs*-57-*Lm*

1 DivIVA (strain BSN344). As controls, GFP-RacA was also imaged in strain BSN340
2 expressing *Bs divIVA* and in strain BSN341 which expresses *Lm divIVA*. Phase contrast
3 images were included for better orientation (bottom row). Scale bar is 5 μ m.

4

5

1 **Table 1:** Plasmids and strains used in this study

Name	relevant characteristics	source*/reference
Plasmids		
pAPNC213	<i>bla aprE5' spc lacI P_{spac} aprE3'</i>	(35)
pAPNC213cat	<i>bla aprE5' cat lacI P_{spac} aprE3'</i>	H. Strahl
pDG9	<i>bla amyE3' spc P_{xyI}-divIVA-gfp amyE5'</i>	(18)
pSG1154	<i>bla amyE3' spc P_{xyI}-gfp amyE5'</i>	(36)
pSH2	<i>bla aprE5' spc lacI P_{spac}-divIVA^{Bs} aprE3'</i>	(18)
pSH3	<i>bla amyE3' spc P_{xyI}-divIVA^{Bs}-gfpA206K amyE5'</i>	(18)
pKT25- <i>racA</i>	<i>kan P_{lac}-cya(T25)-racA</i>	(1)
pUT18- <i>divIVA</i>	<i>bla P_{lac}-cya(T18)-divIVA</i>	(1)
pUT18C- <i>divIVA</i>	<i>bla P_{lac}-cya(T18)-divIVA</i>	(11)
pUT18C- <i>minJ</i>	<i>bla P_{lac}-cya(T18)-minJ</i>	(11)
pUT18C- <i>racA</i>	<i>bla P_{lac}-cya(T18)-racA</i>	(1)
p25-N- <i>divIVA</i>	<i>kan P_{lac}-divIVA-cya(T25)</i>	(1)
p25-N- <i>minJ</i>	<i>kan P_{lac}-minJ-cya(T25)</i>	(11)
pINC3	<i>bla amyE3' spc P_{xyI}-divIVAR131A-gfp amyE5'</i>	this work
pINC12	<i>bla aprE5' spc lacI P_{spac}-divIVA R131A aprE3'</i>	this work
pKK13	<i>bla amyE3' spc P_{xyI}-divIVA^{Bs-57-Lm} amyE5'</i>	this work
pSBLH001	<i>bla P_{lac}-divIVA¹⁻⁴⁵⁹(Δ11)-cya(T18)</i>	this work
pSBLH004	<i>kan P_{lac}-divIVA¹⁻⁴⁵⁹(Δ11)-cya(T25)</i>	this work
pSBLH005	<i>bla P_{lac}-divIVA¹⁻⁴³²(Δ20)-cya(T18)</i>	this work
pSBLH008	<i>kan P_{lac}-divIVA¹⁻⁴³²(Δ20)-cya(T25)</i>	this work
pSBLH036	<i>bla P_{lac}-divIVA¹⁻⁴²⁹(Δ21)-cya(T18)</i>	this work
pSBLH037	<i>bla P_{lac}-divIVA¹⁻⁴¹⁴(Δ26)-cya(T18)</i>	this work
pSBLH038	<i>bla P_{lac}-divIVA¹⁻³⁹⁰(Δ34)-cya(T18)</i>	this work
pSBLH039	<i>kan P_{lac}-divIVA¹⁻⁴²⁹(Δ21)-cya(T25)</i>	this work
pSBLH040	<i>kan P_{lac}-divIVA¹⁻⁴¹⁴(Δ26)-cya(T25)</i>	this work
pSBLH041	<i>kan P_{lac}-divIVA¹⁻³⁹⁰(Δ34)-cya(T25)</i>	this work
pSH19	<i>bla amyE3' spc P_{xyI}-divIVA^{Bs} amyE5'</i>	this work
pSH209	<i>bla amyE3' spc P_{xyI}-divIVA^{Lm} amyE5'</i>	this work
pSH210	<i>bla amyE3' spc P_{xyI}-divIVA^{Lm}-gfp amyE5'</i>	this work
pSH260	<i>bla amyE3' spc P_{xyI}-divIVA^{Lm-71-Bs} amyE5'</i>	this work
pSH261	<i>bla amyE3' spc P_{xyI}-divIVA^{Lm-144-Bs} amyE5'</i>	this work
pSH267	<i>bla amyE3' spc P_{xyI}-divIVA^{Lm-130-Bs} amyE5'</i>	this work
pSH272	<i>bla amyE3' spc P_{xyI}-divIVA^{Lm-83-Bs} amyE5'</i>	this work
pSH278	<i>bla amyE3' spc P_{xyI}-divIVA^{Lm-104-Bs} amyE5'</i>	this work
pSH290	<i>bla amyE3' spc P_{xyI}-divIVA^{Lm-71-Bs}-gfpA206K amyE5'</i>	this work
pSH291	<i>bla amyE3' spc P_{xyI}-divIVA^{Lm-144-Bs}-gfpA206K amyE5'</i>	this work
pSH292	<i>bla amyE3' spc P_{xyI}-divIVA^{Lm-130-Bu}-gfpA206K amyE5'</i>	this work
pSH293	<i>bla amyE3' spc P_{xyI}-divIVA^{Lm-83-Bs}-gfpA206K amyE5'</i>	this work
pSH294	<i>bla amyE3' spc P_{xyI}-divIVA^{Lm-104-Bs}-gfpA206K amyE5'</i>	this work
pSH316	<i>bla aprE5' cat lacI P_{spac}-minJ-gfp aprE3'</i>	this work
pSH317	<i>bla aprE5' cat P_{spac}-minJ-gfp aprE3'</i>	this work
pSH320	<i>bla aprE5' cat P_{divIVA1}-minJ-gfp aprE3'</i>	this work
pSH326	<i>bla amyE3' spc P_{xyI}-divIVA^{Bs-57-lm}-gfp amyE5'</i>	this work
pSH328	<i>bla aprE5' cat P_{divIVA3}-minJ-gfp aprE3'</i>	this work
pSH330	<i>bla aprE5' spc lacI P_{spac}-divIVA^{Bs}R102K aprE3'</i>	this work
pSH331	<i>bla aprE5' spc lacI P_{spac}-divIVA^{Bs}R102E aprE3'</i>	this work
pSH334	<i>bla aprE5' spc lacI P_{spac}-divIVA^{Bs}ΔC34 aprE3'</i>	this work
pSH335	<i>bla aprE5' cat lacI P_{spac}-divIVA^{Bs} aprE3'</i>	this work
pSH336	<i>bla aprE5' cat lacI P_{spac}-divIVA^{Bs}R102K aprE3'</i>	this work
pSH337	<i>bla aprE5' cat lacI P_{spac}-divIVA^{Bs}R102E aprE3'</i>	this work
pSH340	<i>bla aprE5' cat lacI P_{spac}-divIVA^{Bs}ΔC34 aprE3'</i>	this work
pSH354	<i>bla amyE3' spc P_{xyI}-divIVA^{Lm}-gfpA206K amyE5'</i>	this work
pSH355	<i>bla amyE3' spc P_{xyI}-divIVA^{Bs-57-lm}-gfpA206K amyE5'</i>	this work
B. subtilis strains		
168	<i>trpC2</i>	
168 (pSG4916)	168 <i>racA::pSG4916(P_{xyI}-gfp-racA' cat)</i>	(8)

Name	relevant characteristics	source*/reference
4041	168 <i>divIVA::tet</i>	(18)
BSN5	168 <i>aprE::P_{spac}-divIVA spc lacI divIVA::tet</i>	(18)
SB002	168 <i>amyE::P_{xyI}-minJ-gfp spc minJ::tet</i>	(37)
BSN51	168 <i>amyE::P_{xyI}-divIVA^{Bs} spc divIVA::tet</i>	this work
BSN238	168 <i>amyE::P_{xyI}-divIVA^{Lm} spc divIVA::tet</i>	this work
BSN274	168 <i>amyE::P_{xyI}-divIVA^{Lm-144-Bs} spc divIVA::tet</i>	this work
BSN278	168 <i>amyE::P_{xyI}-divIVA^{Lm-130-Bs} spc divIVA::tet</i>	this work
BSN287	168 <i>amyE::P_{xyI}-divIVA^{Lm-83-Bs} spc divIVA::tet</i>	this work
BSN288	168 <i>amyE::P_{xyI}-divIVA^{Lm-104-Bs} spc divIVA::tet</i>	this work
BSN294	168 <i>amyE::P_{xyI}-divIVA^{Lm-71-Bs}-gfpA206K spc divIVA::tet</i>	this work
BSN295	168 <i>amyE::P_{xyI}-divIVA^{Lm-144-Bs}-gfpA206K spc divIVA::tet</i>	this work
BSN296	168 <i>amyE::P_{xyI}-divIVA^{Lm-130-Bs}-gfpA206K spc divIVA::tet</i>	this work
BSN297	168 <i>amyE::P_{xyI}-divIVA^{Lm-83-Bs}-gfpA206K spc divIVA::tet</i>	this work
BSN298	168 <i>amyE::P_{xyI}-divIVA^{Lm-104-Bs}-gfpA206K spc divIVA::tet</i>	this work
BSN308	168 <i>aprE::P_{spac}-minJ-gfp cat lacI</i>	this work
BSN313	168 <i>aprE::P_{spac}-divIVA R131A spc lacI divIVA::tet</i>	this work
BSN316	168 <i>amyE::P_{xyI}-divIVA^{Lm-71-Bs} spc divIVA::tet</i>	this work
BSN317	168 <i>aprE::P_{spac}-minJ-gfp cat</i>	this work
BSN321	168 <i>amyE::P_{xyI}-divIVA^{Bs-57-Lm} spc divIVA::tet</i>	this work
BSN332	168 <i>aprE::P_{divIVA3}-minJ-gfp cat</i>	this work
BSN333	168 <i>aprE::P_{divIVA3}-minJ-gfp cat divIVA::tet</i>	this work
BSN334	168 <i>aprE::P_{divIVA3}-minJ-gfp cat amyE::P_{xyI}-divIVA^{Bs} spc divIVA::tet</i>	this work
BSN335	168 <i>aprE::P_{divIVA3}-minJ-gfp cat amyE::P_{xyI}-divIVA^{Lm} spc divIVA::tet</i>	this work
BSN336	168 <i>aprE::P_{divIVA3}-minJ-gfp cat amyE::P_{xyI}-divIVA^{Lm-104-Bs} spc divIVA::tet</i>	this work
BSN338	168 <i>aprE::P_{divIVA3}-minJ-gfp cat amyE::P_{xyI}-divIVA^{Bs-57-Lm} spc divIVA::tet</i>	this work
BSN340	168 <i>racA::pSG4916(P_{xyI}-gfp-racA'cat) amyE::P_{xyI}-divIVA^{Bs} spc divIVA::tet</i>	this work
BSN341	168 <i>racA::pSG4916(P_{xyI}-gfp-racA'cat) amyE::P_{xyI}-divIVA^{Lm} spc divIVA::tet</i>	this work
BSN342	168 <i>racA::pSG4916(P_{xyI}-gfp-racA'cat) amyE::P_{xyI}-divIVA^{Lm-104-Bs} spc divIVA::tet</i>	this work
BSN344	168 <i>racA::pSG4916(P_{xyI}-gfp-racA'cat) amyE::P_{xyI}-divIVA^{Bs-57-Lm} spc divIVA::tet</i>	this work
BSN356	168 <i>aprE::P_{spac}-divIVA^{Bs} cat lacI divIVA::tet</i>	this work
BSN357	168 <i>aprE::P_{spac}-divIVA^{Bs} R102K cat lacI divIVA::tet</i>	this work
BSN358	168 <i>aprE::P_{spac}-divIVA^{Bs} R102E cat lacI divIVA::tet</i>	this work
BSN360	168 <i>aprE::P_{spac}-divIVA^{Bs} ΔC34 cat lacI divIVA::tet</i>	this work
BNS372	168 <i>amyE::P_{xyI}-divIVA^{Bs-57-Lm}-gfpA206K spc divIVA::tet</i>	this work
BSN373	168 <i>amyE::P_{xyI}-divIVA^{Lm}-gfpA206K spc divIVA::tet</i>	this work

1

2

1 **Table 2:** Oligonucleotides used in this study.

Name	sequence (5'→3')
25_N_18_F	CCGGGTACCGAGCTCGAATTCA
<i>divIVA</i> _11_B2H_R	GCGGGTACCTCAAGGAGATGATCCCA
<i>divIVA</i> _19_B2H_R	GCGGGTACCAATTTTCAGAAGATCAAG
<i>divIVA</i> _21_R	GCGGGTACCAGAAGATCAAGCTGAGCT
<i>divIVA</i> _26_R	GCGGGTACCGCTTCAATCAGCATTG
<i>divIVA</i> _34_R	GCGGGTACCGTTCTGAACACTTTAGAC
SHW109	CTTAGGTACCAAGCTAGTAACTATGGTAGAATG
SHW110	GCGCTCGAGTTAACGTTCTTCAGATTCAGCTG
SHW111	GCGCTCGAGACGTTCTTCAGATTCAGCTG
SHW180	CGAAGTAAATGACTTCCTCGATC
SHW184	CTTAACTAGTTTTGTATAGTTTCATCCATGCC
SHW237	GAACGTTTAGGTCATTTTACAAACATTGAGGAGACATTGAATAAATC
SHW238	GTGGAAGCACAAATGGATTTAATTAATAAATGACGATTGGGATCATC
SHW247	CGTCAATCCAAAGTATTCGGTACACGTTTCCAAATGCTGATTG
SHW265	CAAACAGCTGCCGAAGAAGTGAAACGCAATTCTCAAAAAGAAGCAAAG
SHW266	GCAGAAAAAATGCTGACCGAATTATCAACGAATCGTTATCAAAATC
SHW304	AAAGGAAGGACTTGATATCGAATTCC
SHW305	TATCAAGTCCTTCTTTTCTCAAATAC
SHW342	ATATGTCGACACATAAAAATGCATCTAGAAAGGAG
SHW343	GCGCGGATCCTTATTTGTATAGTTTCATCCATGCC
SHW349	TTGCGCTCACATCAAATCGTCTCCCTCCG
SHW350	GATTTGATGTGAGCGCAACGCAAGCTTC
SHW354	GTCGTATGGAGGTGCTAGATATGCCATTAACGCCAAATGATATTC
SHW355	GTTTCTTCAATGTTTGTAATAATGACCGATTCTTTTCATCAAGCTCATTG
SHW356	GACACCTCGAGCATGATGCCACCTCCATTTTTAC
SHW357	TGATGCCACCTCCATTTTTTACATTTC
SHW358	AAATGGAGGTGGCATCATGCTCGAGG
SHW366	GAAGAACGTGGACTCGAGGTGACGGTATC
SHW367	GACCTCGAGTCCACGTTCTTCAGATTCAGCTG
SHW378	CGCTGATAAAAATTATCAACGAATCG
SHW379	GATAATTTTATCAGCGTTTTTCTCC
SHW380	CGCTGATGAAATTATCAACGAATC
SHW381	GATAATTTTCATCAGCGTTTTTCTCC
SHW386	TCAGAACATAATTCCAAATGCTGATTGAAG
SHW387	ATTTGGAATTATGTTCTGAACACTTTAGAC
SHW425	CACAATCTAAACTTTCCAAAGATCCCAACG
SHW426	GGAAAGTTTAGATTGTGTGGACAGGTAATG
SV23	GAAAAGGAATAACTTGATATCGAATTTC
SV24	GATATCAAGTTATTCCTTTTCTCAAATAC
SV81	CGCGCGAGCTCTTATTCCTTTTCTCAAATACAGC
SV98	CTTAGGTACCTTGCCGGTGCAGCTTAAC
SV123	CGGGATCCAAAATGGAGGTGGCATCATGCCATTAACGCCAAATG
R131A_fw	TCAGAACAGCTTTCCAAATGCTGATTG
R131A_rev	TTTGAAAAGCTGTTCTGAACACTTTAG

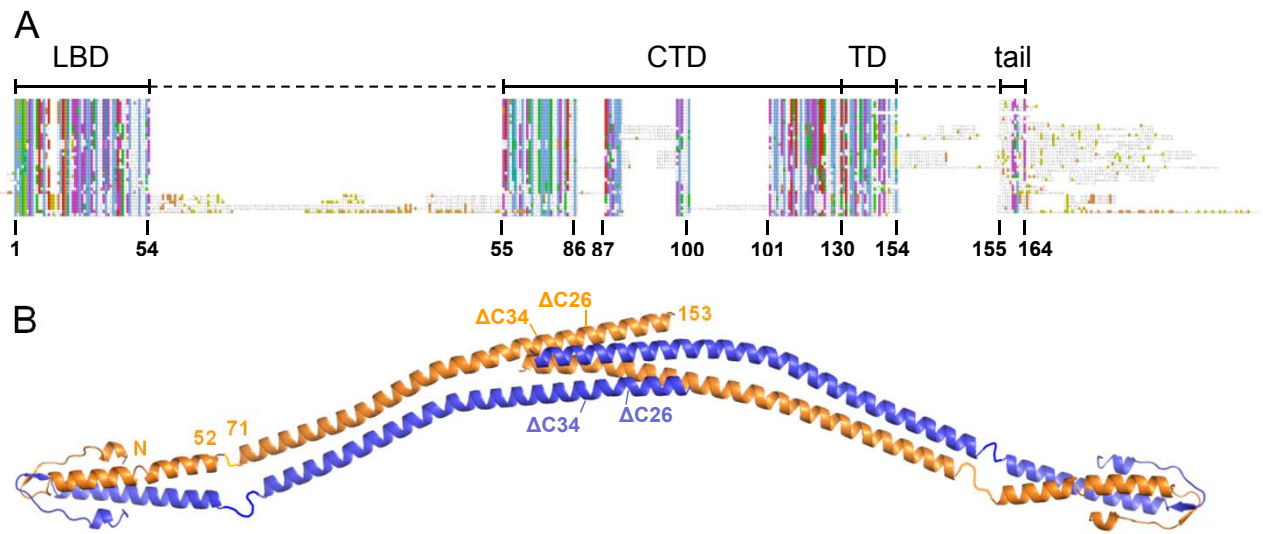
2

3

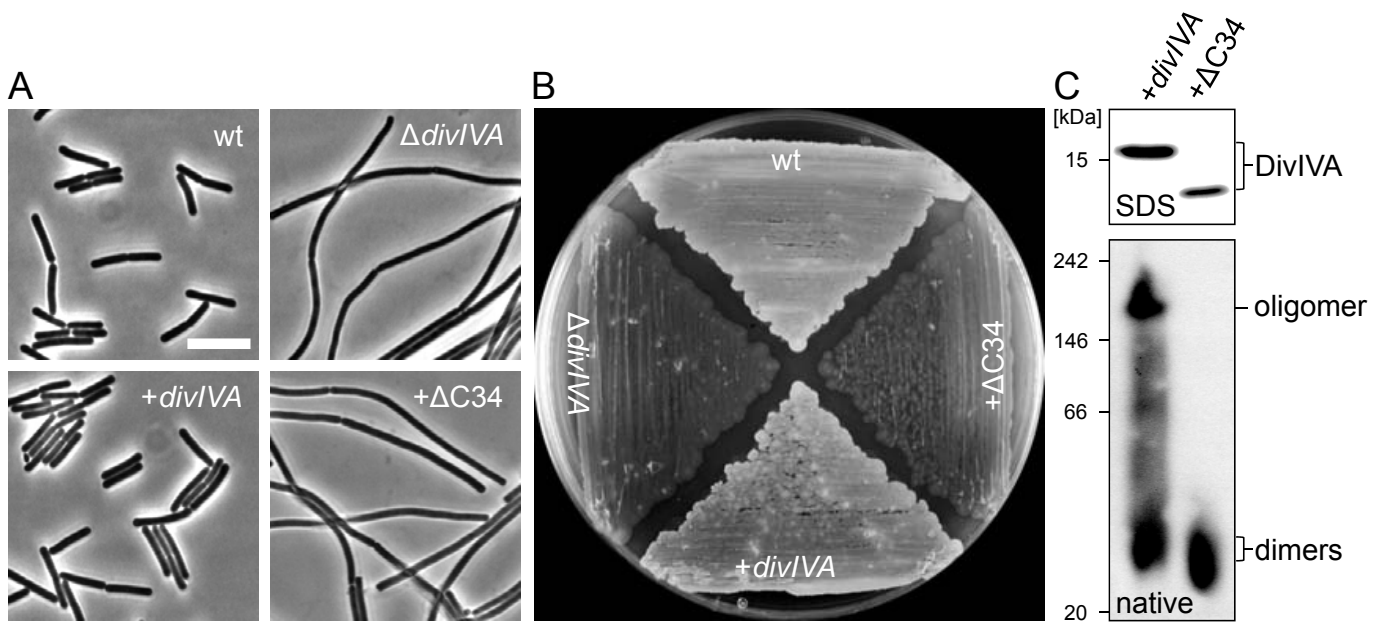
1 **Table 3:** Bacterial two-hybrid analysis of C-terminal DivIVA truncation mutants regarding
 2 their ability to interact with full-length DivIVA, MinJ, and RacA.

DivIVA	C-terminal protein sequence*	DivIVA	MinJ	RacA
wt	LKKQSKVFRTRFQMLIEAQLDLLKNDDWDHLLLEYEVDVAVFEEKE-164	+	+	+/-
Δ11	LKKQSKVFRTRFQMLIEAQLDLLKNDDWDHLLLE-153	+	+	-
Δ20	LKKQSKVFRTRFQMLIEAQLDLLK-144	+	+	-
Δ21	LKKQSKVFRTRFQMLIEAQLDLL-143	+	+	-
Δ26	LKKQSKVFRTRFQMLIEA-138	+/-	+/-	-
Δ34	LKKQSKVFR-130	+/-	+/-	-

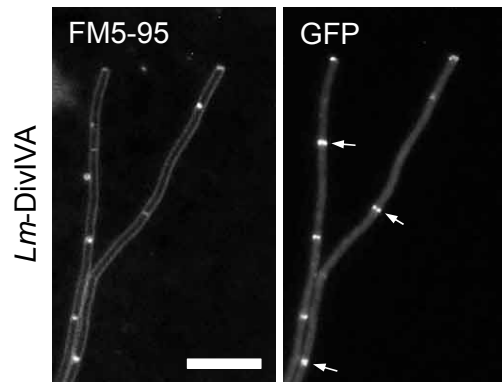
3 * Starting from position 121. The shadowed sequence stretch corresponds to the DivIVA tetramerization
 4 domain. The position of the last amino acid in the truncated DivIVA proteins is given at the end of the sequence
 5 Symbols: + = dark blue, +/- = light blue, - = white. For comparison see Fig. S1.



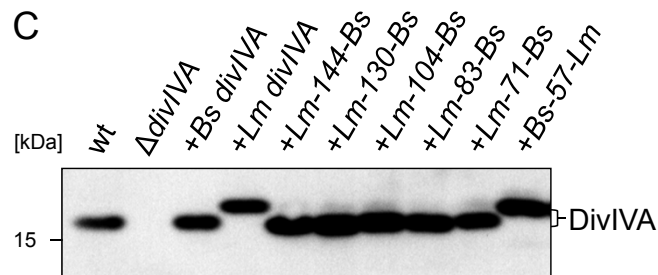
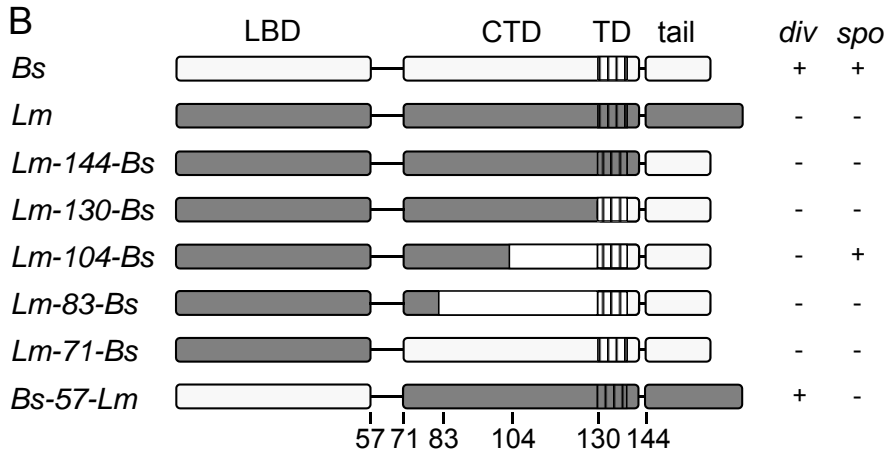
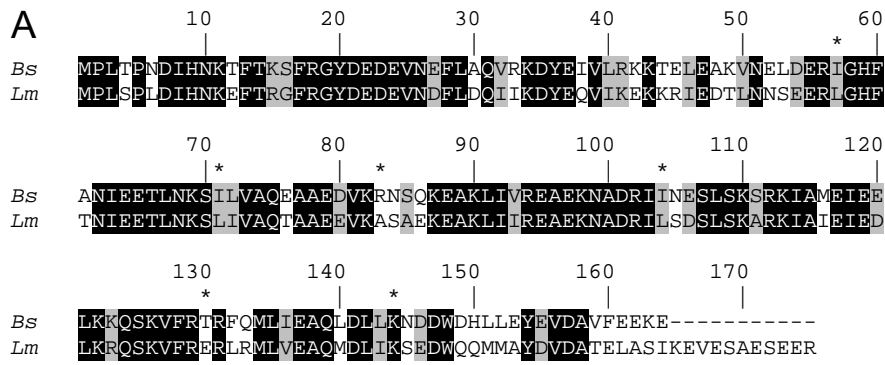
van Baarle *et al.*, Figure 1



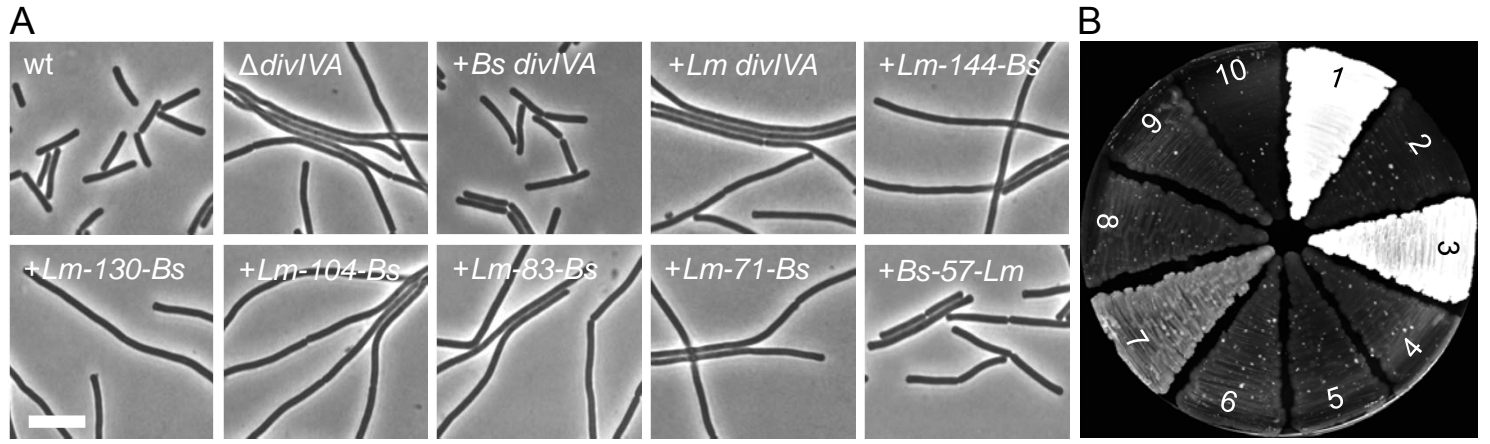
van Baarle *et al.*, Figure 2



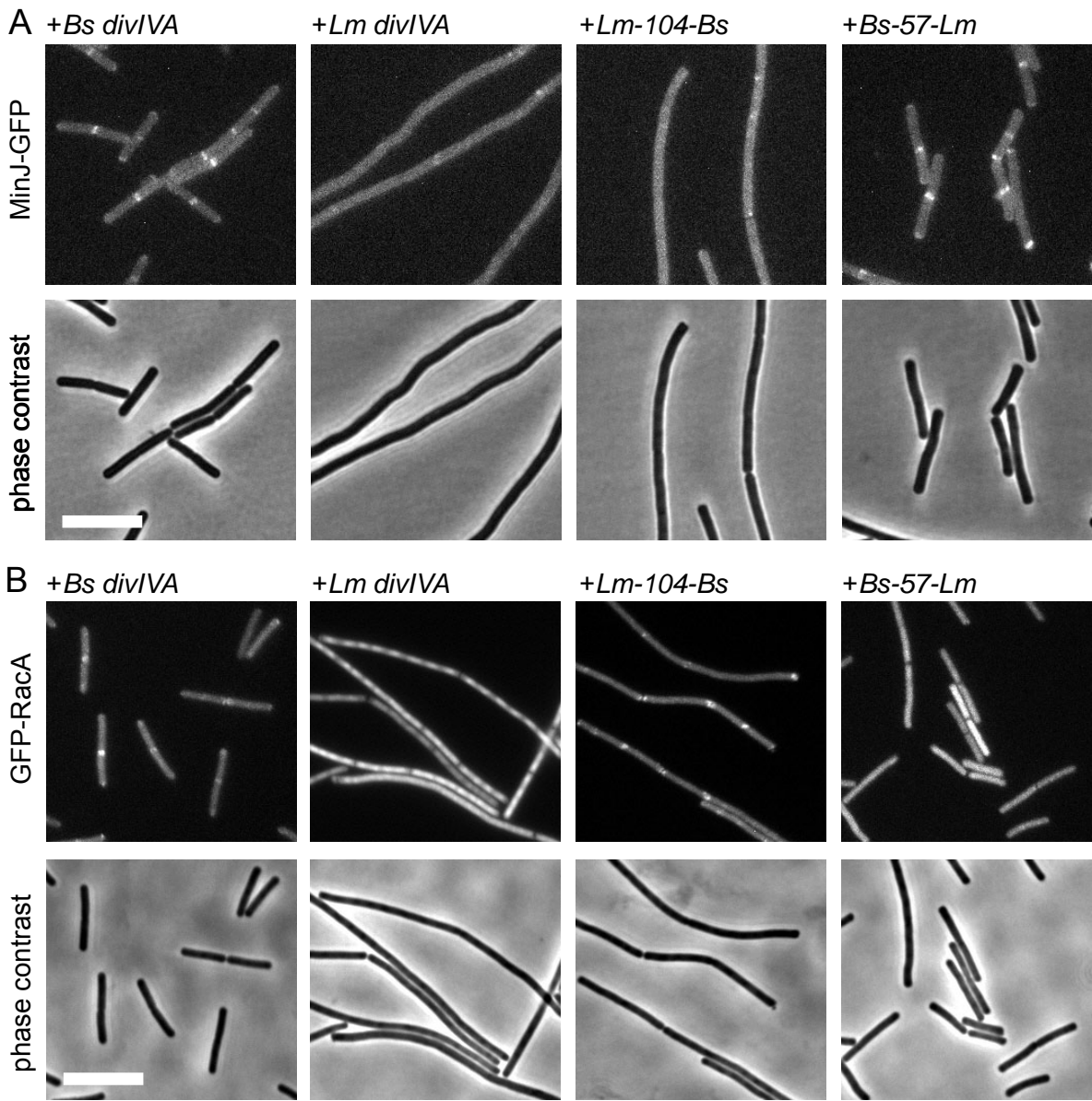
van Baarle *et al.*, Figure 3



van Baarle *et al.*, Figure 4



van Baarle *et al.*, Figure 5



van Baarle *et al.*, Figure 6

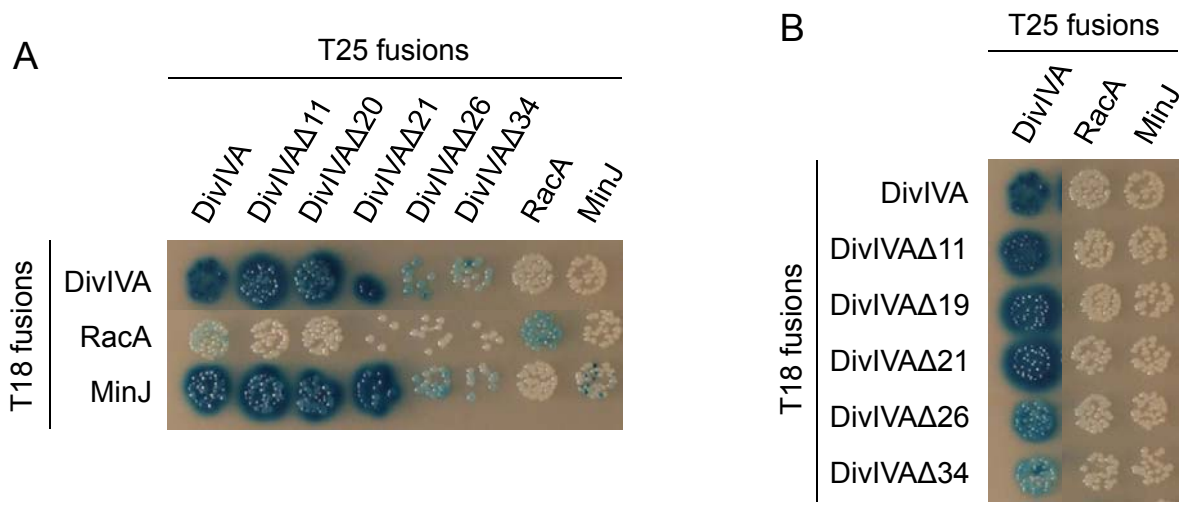


Fig. S1: Bacterial two hybrid analysis of the *DivIVA* interaction to *MinJ* and *RacA*. (A) The T25 plasmids p25-N-*divIVA* (full length *DivIVA*), pSBLH004 (*DivIVA*Δ11), pSBLH008 (*DivIVA*Δ20), pSBLH039 (*DivIVA*Δ21), pSBLH040 (*DivIVA*Δ26), and pSBLH041 (*DivIVA*Δ34), were co-transformed with the T18 plasmids pUT18C-*divIVA*, pUT18C-*racA*, and pUT18C-*minJ* in the *E. coli* strain BTH101 and aliquots of the transformation mixture were spotted onto nutrient agar plates containing ampicillin, kanamycin, IPTG and X-Gal (for details see materials and methods section). Images were taken after 40 h of incubation at 30°C. The T25 plasmids pKT25-*racA* and p25-N-*minJ* were used as self-interaction controls. (B) Reciprocal bacterial two hybrid experiment (taken from the same plate) in which the T25 plasmids p25-N-*divIVA*, pKT25-*racA*, and p25-N-*minJ* were co-transformed into BTH101 along with pUT18 plasmids containing the *DivIVA* truncation series. This experiment confirmed the reduced interaction of *DivIVA*Δ26 and *DivIVA*Δ34 with full-length *DivIVA*. However, T25 fusions of *RacA* and *MinJ* did not reveal any interactions with *DivIVA* in this orientation.

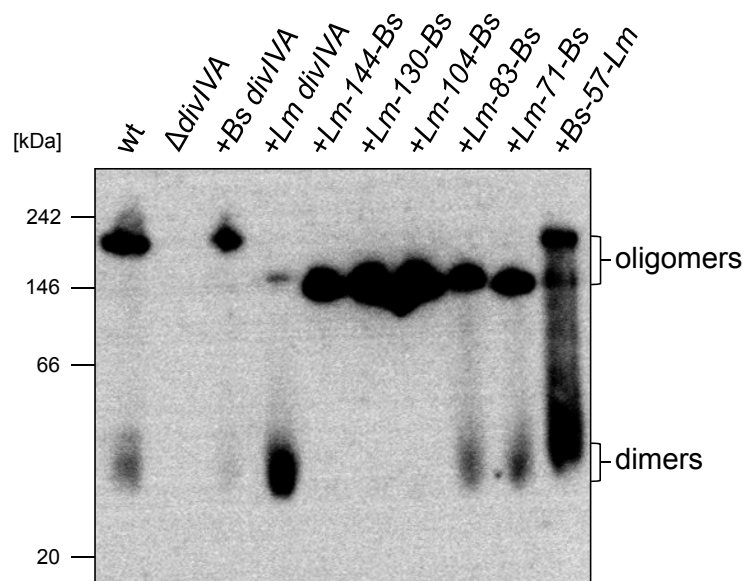


Fig. S2: Western blot after blue native PAGE to analyze oligomerization of chimeric DivIVA proteins. Strains expressing chimeric DivIVA proteins (BSN274: +*Lm*-144-*Bs divIVA*; BSN278: +*Lm*-130-*Bs divIVA*; BSN288: +*Lm*-104-*Bs divIVA*; BSN287: +*Lm*-83-*Bs divIVA*; BSN316: +*Lm*-71-*Bs divIVA*; BSN321: +*Bs*-57-*Lm divIVA*) were grown in LB broth supplemented with 0.5% xylose at 37°C and harvested in mid-logarithmic growth phase. Cell extracts were subjected to blue native PAGE, blotted onto a PVDF membrane and DivIVA proteins were immunostained using the anti-DivIVA antiserum. Strains 168 (wt), 4041 (Δ *divIVA*) and strains expressing the *B. subtilis* (BSN51) or the *L. monocytogenes divIVA* gene (BSN238) were used as controls. Please note that differences in the apparent molecular weight of the different DivIVA oligomers are explained by pI differences between *Bs* (pI 5.03) and *Lm* DivIVA (pI 4.77). During electrophoresis, which was performed at pH 7.5, *Lm* DivIVA is more negatively charged as compared to *Bs* DivIVA and therefore runs faster through the gel even though its monomer has the higher theoretical molecular weight. Moreover, the pI values of the C-terminal domains of both proteins are nearly identical (*Bs* CTD: 4.93; *Lm* CTD: 4.80) whereas those of the N-terminal lipid binding domains are rather different (*Bs* LBD: 5.27; *Lm* LBD: 4.72). This explains why all chimeras containing the *Lm* LBD reveal the same apparent oligomer molecular weight as *Lm* DivIVA, whereas the *Bs*-57-*Lm* oligomer runs at the same position as *Bs* DivIVA.

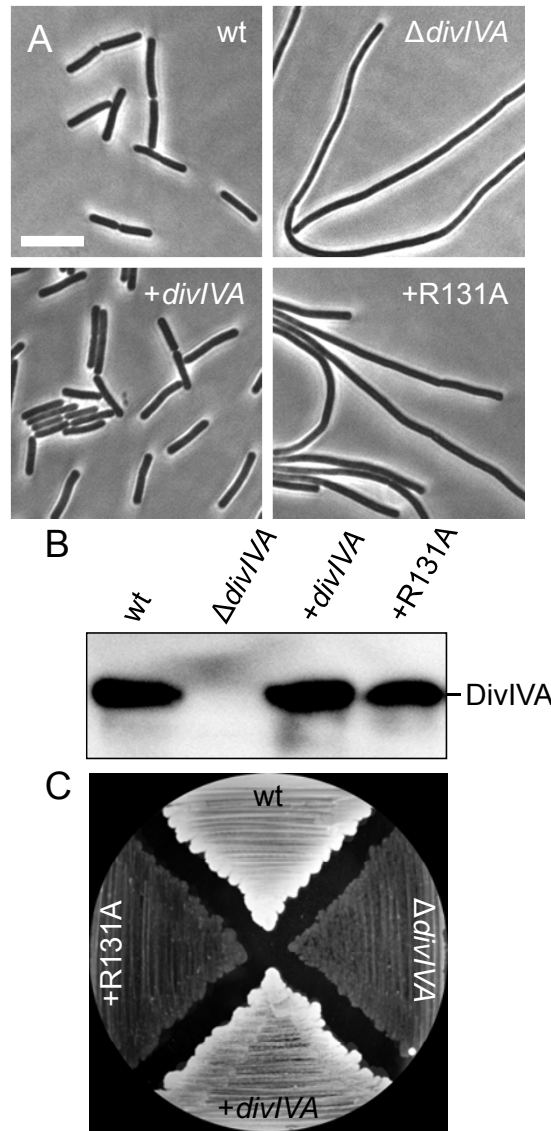


Fig. S3: A mutation in the tetramerisation domain (R131A) that causes an inactive *Bs* DivIVA protein. (A) Phase contrast micrographs obtained on cultures that were cultivated in LB broth containing 1 mM IPTG at 37°C during mid-logarithmic growth. Strains used were 168 (wt), 4041 ($\Delta divIVA$), BSN5 (+*divIVA*) and BSN313 (+R131A). Scale bar is 5 μ m. (B) Western blot on cell extracts of the same set of strains. DivIVA was visualised using the polyclonal rabbit anti-DivIVA antiserum. (C) The *divIVAR131A* mutant (strain BSN313) reveals a sporulation defect. Sporulation was assayed in a plate assay as described in the legend of Fig. 3B.

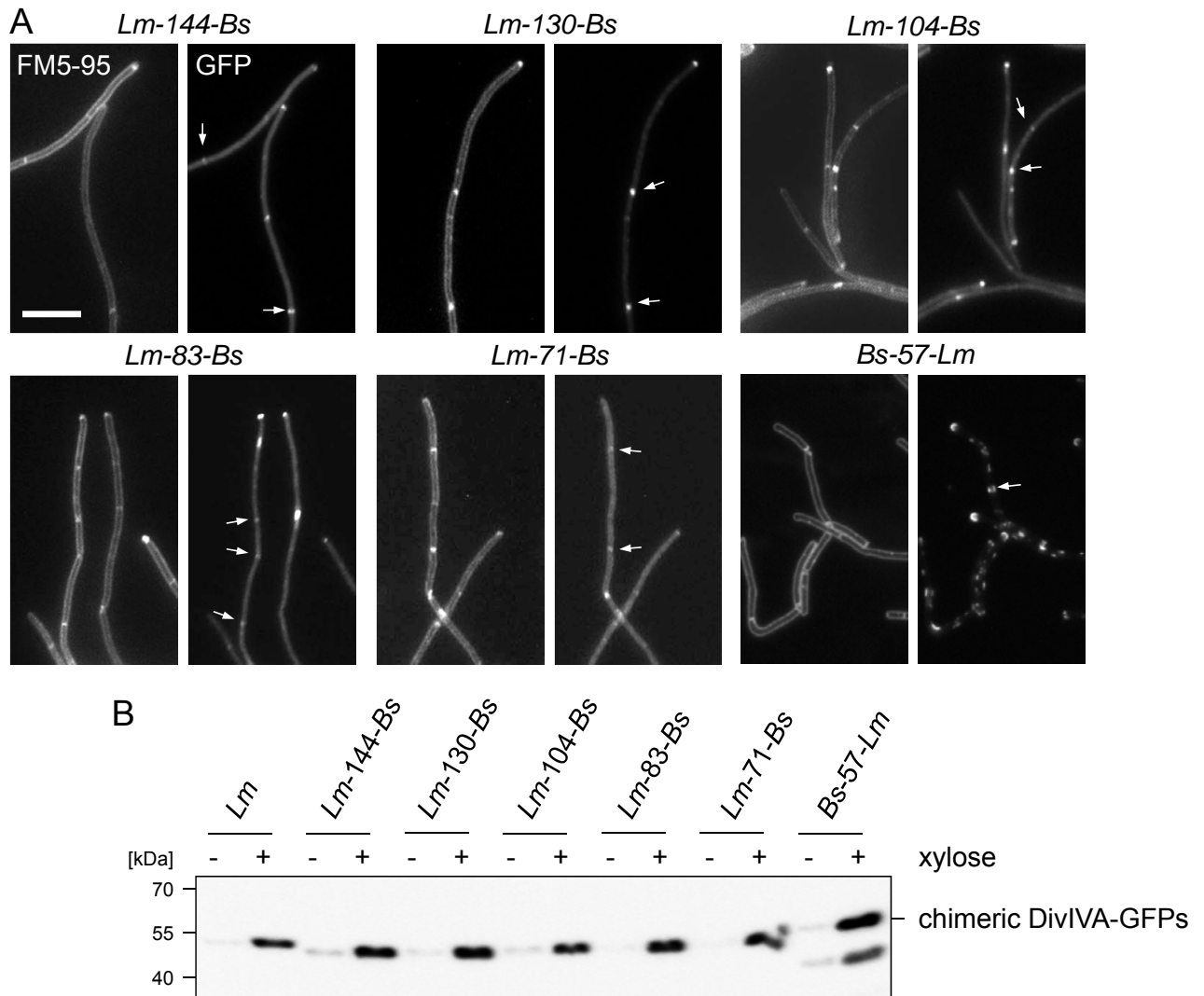


Fig. S4: Subcellular localisation of chimeric DivIVA proteins in a *B. subtilis* $\Delta divIVA$ background. Strains BSN294 (DivIVA^{Lm-71-Bs}-GFP), BSN295 (DivIVA^{Lm-144-Bs}-GFP), BSN296 (DivIVA^{Lm-130-Bs}-GFP), BSN297 (DivIVA^{Lm-83-Bs}-GFP), BSN298 (DivIVA^{Lm-104-Bs}-GFP), and strain BSN372 (DivIVA^{Bs-57-Lm}-GFP) were grown in LB supplemented with 0.5% xylose. DivIVA localisation patterns were analysed by epifluorescence microscopy (right images), and for orientation, FM5-95 stained images (left panels) were taken in parallel. Scale bar is 5 μ m, septal DivIVA-GFP signals are indicated by arrows. All DivIVA-GFP fusions contain the *gfpA206K* mutation preventing GFP dimerization. (B) Western blot to demonstrate full-length expression of chimeric DivIVA-GFP proteins. Strains expressing chimeric DivIVA-GFP fusions were grown in LB broth containing or not containing 0.5% xylose to mid-logarithmic growth phase, total cellular proteins were isolated and subjected to SDS-PAGE and subsequent Western blotting. DivIVA-GFP fusion proteins were visualised using the polyclonal anti-GFP antiserum. Strains were as in panel A, but BSN373 (expressing *Lm* DivIVA-GFP) was also included. For convenience the names of the respective DivIVA chimeras are indicated above the blot. Please note that DivIVA^{Bs-57-Lm}-GFP shows some proteolytic degradation.

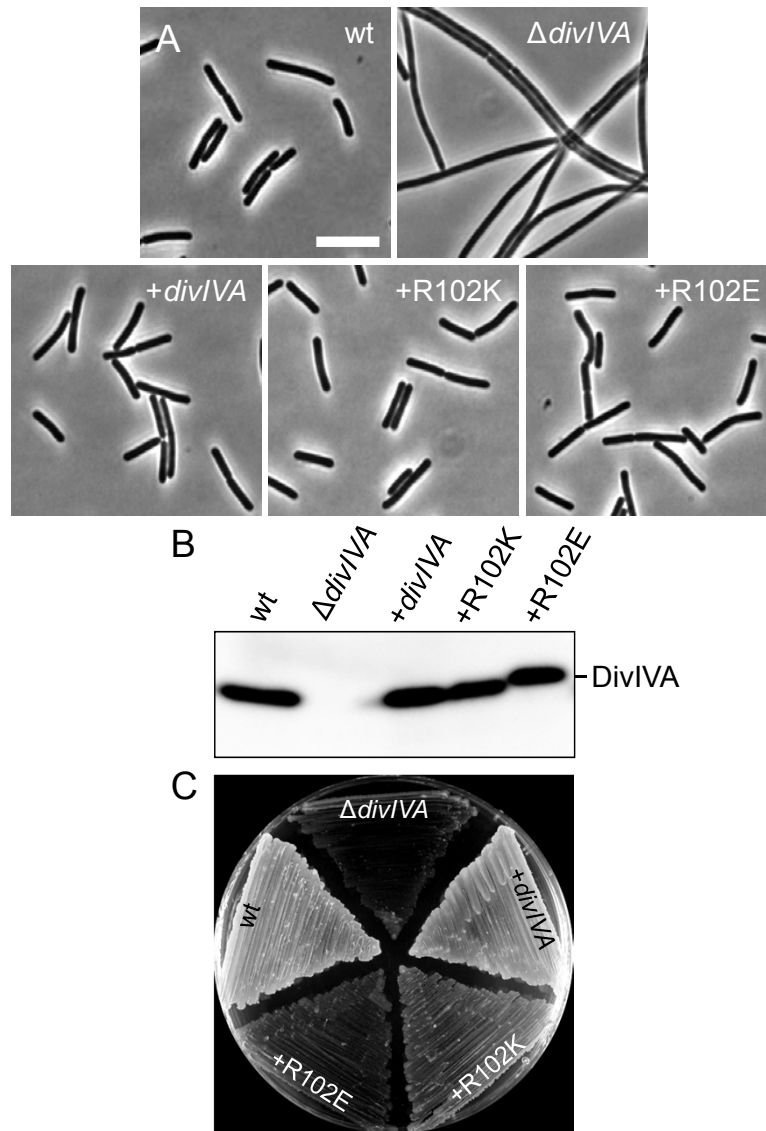


Fig. S5: Mutations of R102 in *Bs divIVA* cause a *div⁺ spo⁻* phenotype. (A) Phase contrast micrographs obtained on cultures that were cultivated in LB broth containing 1 mM IPTG (where necessary) at 37°C during mid-logarithmic growth. Strains used for this experiment were 168 (wt), 4041 ($\Delta divIVA$), BSN356 (+*divIVA*), BSN357 (+R102K), and BSN358 (+R102E). Scale bar is 5 μ m. (B) Western blot on cell extracts of the same set of strains. DivIVA was visualised using the polyclonal rabbit anti-DivIVA antiserum. (C) Sporulation activity of the R102 mutants. Sporulation was assayed in a plate assay as described in the legend of Fig. 3. Please note that the sporulation defect of the phospho-ablative R102K mutant was less pronounced than that of the phospho-mimetic R102E allele.